

Effects of Solution Composition and pH on the Reductive Dechlorination of Hexachloroethane by Iron Sulfide

ELIZABETH C. BUTLER AND
KIM F. HAYES*

Department of Civil and Environmental Engineering,
University of Michigan, Ann Arbor, Michigan 48109-2125

Transition metal sulfide minerals are under investigation as potentially important abiotic reductants for chlorinated organic pollutants in anaerobic environments. This paper describes parametric rate studies done to evaluate the influence of environmental variables such as pH and ionic and organic solution composition on the reductive dechlorination of hexachloroethane (HCA) by FeS (poorly crystalline mackinawite). Results indicate that the reaction takes place at the mineral surface and is strongly pH-dependent. The influence of pH was explained by an acid/base equilibrium between two FeS surface species with different reactivities. Tetrachloroethylene was the principal reaction product, with pentachloroethane (PCA) as a minor intermediate and trichloroethylene, *cis*-1,2-dichloroethylene, and acetylene as minor products. Detection of PCA and the insensitivity of the reaction to numerous inorganic and organic solution species is consistent with an outer-sphere HCA dechlorination pathway involving two successive one-electron transfers. 2,2'-Bipyridine and 1,10-phenanthroline significantly increased the rate of HCA dechlorination by FeS, which was explained by the participation of delocalized π^* molecular orbitals in the electron-transfer reaction. Cysteine and methionine were found to slow, but not stop, the reaction rate, and this was attributed to adsorption of thiol and sulfide functional groups to FeS surface iron atoms, causing an energetic or steric barrier to electron transfer. Rapid dechlorination rates and the insensitivity of the dechlorination reaction to numerous ionic and organic species suggest that FeS-mediated reductive dechlorination may be an important transformation pathway in natural systems.

Introduction

National drinking water surveys indicate that chlorinated organic compounds, many of which are known or suspected human carcinogens, are widespread at trace levels in U.S. drinking water supplies (1). Transition metal sulfides such as FeS are likely to be relevant reductants for such compounds in anaerobic environments, since several studies have found that the majority of the reduction capacity in natural waters is associated with sediment and aquifer solids (2–5), and this solid-phase reduction capacity has been attributed in part to Fe(II) and Mn(II) minerals and sulfide species (4). FeS, produced primarily through the biologically mediated reduction of sulfate to sulfide and subsequent reaction of

sulfide with available iron species, is observed to precipitate on the surface of anoxic clay soils (6). Although other iron sulfide minerals (e.g., greigite, pyrite, marcasite) may eventually form, the mineral mackinawite is the initial FeS precipitate and a metastable phase under sulfate-reducing conditions (7). Mackinawite has been identified along with amorphous FeS in a number of aquatic systems (8–10).

A number of recent studies have examined dechlorination reactions mediated by transition metal sulfides and disulfides such as FeS (11–19), and they point to the potential importance of these minerals in the abiotic transformation of chlorinated pollutants in natural systems. Some of the more detailed of these studies have addressed dechlorination of carbon tetrachloride (CT) by the iron disulfides pyrite and marcasite (12, 14). In the case of pyrite, kinetics characteristic of a surface reaction were observed, and it was concluded that CT transformation was due to surface disulfide functional groups (14). While one study (13) reported no effective transformation of CT in the presence of precipitated FeS, these results differ significantly from other reported results (15, 18), and it appears that FeS may be effective in CT degradation. Degradation of hexachloroethane (HCA), tetrachloroethylene (PCE), and trichloroethylene (TCE) by pyrite, FeS, and nickel and copper sulfides has been observed under certain conditions (11, 16), and metal sulfide reactivity has been related to the separation between transition metal d orbitals and sulfur p orbitals for several of these minerals (16). Based on surface X-ray photoelectron spectroscopy, it has been suggested that trichloroethylene (TCE) reductive dechlorination in the presence of FeS (troilite) is due to surface-bound Fe(II) and not S(–II) species (17).

The experiments described here evaluate the influence of environmental variables such as pH, ionic composition, and the presence of organic molecules similar to those found in natural waters on the rates and products of reductive dechlorination of HCA by FeS. The goal of these experiments was to assess in a more detailed manner the characteristics and reactivities of the species involved in dechlorination reactions mediated by FeS, thereby allowing better assessment of the fate of chlorinated organic pollutants in anaerobic natural waters. Because of its existence in anaerobic environments, mackinawite was the FeS mineral studied here. HCA was chosen for study since it represents a major class of drinking water pollutant (two-carbon chlorinated organic compounds) and because it was expected to undergo rapid dechlorination due to its high standard reduction potential, allowing completion of a number of parametric studies in a reasonable period of time.

Experimental Section

Anaerobic Conditions. All experiments were conducted in polyethylene glovebags (Instruments for Research and Industry, Cheltenham, PA) that were evacuated with a vacuum pump and refilled with N₂ (99.998% purity) a total of three times prior to use and twice daily to remove oxygen that diffused into the glovebag. All aqueous solutions were deoxygenated by placing them in serum bottles and sparging with N₂ for 20 min, after which time the bottles were immediately crimp-sealed with Teflon-lined rubber stoppers and aluminum crimp seals.

Chemicals. All chemicals were reagent or ACS grade and were used as received. Water was distilled and then purified using a Milli-Q Plus water system (Millipore Corp., Bedford MA). FeS was prepared in a manner adapted from Rickard (20). A total of 1200 mL of approximately 1.1 M Na₂S was slowly added to 2 L of 0.57 M FeCl₂ inside an anaerobic

* To whom correspondence should be addressed. Phone: (734) 763–9661; fax: (734) 763–2275; e-mail: ford@engin.umich.edu.

TABLE 1. Observed First-Order Rate Constants as a Function of pH and FeS Concentration^a

FeS (g/L)	pH ^b	ionic strength (M) ^b	k_{obs} (h ⁻¹) ^c
5	7.7	0.05	0.0603 ± 0.0036
10	7.8	0.05	0.0726 ± 0.0079
25	7.8	0.05	0.086 ± 0.012
100	7.8	0.1	0.533 ± 0.072
100	7.1	0.1	0.50 ± 0.15
100	8.3	0.1	0.948 ± 0.078
100	8.8	0.1	1.43 ± 0.21
100	9.5	0.1	3.21 ± 0.51

^a The initial aqueous HCA concentration was approximately 16 μ M.

^b Solution pH and ionic strength were established using NaCl and HCl. No pH buffer was present. ^c Values of k_{obs} were calculated by iterative solution of the first-order rate law for HCA disappearance, i.e., $[\text{HCA}] = [\text{HCA}]_0 e^{-k_{\text{obs}} t}$, using a statistical fitting program. Data were typically collected over three half-lives. Uncertainties represent 95% confidence intervals.

glovebag. The resulting slurry was mixed for 3 days and then decanted into polypropylene bottles that were tightly sealed and centrifuged at 8000 rpm for 10 min. The supernatant was discarded; fresh deoxygenated water was added; and the bottles were shaken, equilibrated, and recentrifuged a total of eight times over several days. This procedure was done entirely in an anaerobic glovebag except for brief periods when the tightly sealed polypropylene bottles were centrifuged. The FeS was then freeze-dried under vacuum and stored under N₂ at all times except for brief periods when it was weighed. FeS was characterized by powder X-ray diffraction as poorly crystalline mackinawite, and the specific surface area was determined to be 0.05 m²/g by BET analysis of krypton adsorption. Although it is possible that there was some oxidation of the FeS surface during the preparation and weighing as described above, the reactivity of this material with respect to HCA reductive dechlorination as well as its characteristic black color and sulfide odor indicate that it remained largely unoxidized during these procedures.

Preparation and Analysis of Samples. Kinetic experiments were conducted in 5 mL flame-sealed glass ampules (21, 22). FeS was added to the appropriate ionic or organic medium (listed in Tables 1–3) inside the anaerobic glovebag, and 4.95 mL of the resulting FeS slurry was added to each ampule with an automatic pipet while the slurry was mixed vigorously on a magnetic stir plate. Ampules were then covered with a double layer of Saran Wrap (Dow Brands, Indianapolis, IN) (22) and fastened with a short piece of plastic tubing. For experiments where pH was an experimental variable (Table 1), the pH of the FeS slurry was adjusted with HCl or NaOH and measured in the glovebag after equilibration.

After equilibration, ampules were removed from the glovebag (with the Saran Wrap serving as a temporary barrier to oxygen diffusion), and 50 μ L of a concentrated HCA stock solution that had been prepared in N₂-sparged methanol was injected through the Saran Wrap, well below the surface of the liquid. The resulting aqueous solution contained 1% methanol by volume. With the exception of certain data shown in Table 2, the stock solution concentration was 0.002 M HCA, and the resulting initial aqueous HCA concentration was approximately 16 μ M due to partitioning of HCA to the ampule headspace. Ampules were then quickly sealed in a methane–oxygen flame and placed in the dark on an Eberbach (Ann Arbor, MI) model 6010 reciprocating shaker at a shaking frequency of 180 excursions per minute in a temperature-controlled chamber at 25 °C. For kinetic experiments of duration longer than approximately 2 days, aqueous solutions were sterilized prior to preparing samples

TABLE 2. Observed Initial Rates and First-Order Rate Constants as a Function of Initial HCA Concentration for 10 g/L FeS, 0.1 M Tris Buffer, and pH 8.3

$[\text{HCA}]_0$ (M)	initial rate (M h ⁻¹) ^a	k_{obs} (h ⁻¹) ^b
1.67×10^{-6}	$-1.64 (\pm 0.36) \times 10^{-7}$	0.1501 ± 0.0080
3.32×10^{-6}	$-4.38 (\pm 3.23) \times 10^{-7}$	0.134 ± 0.026
6.67×10^{-6}	$-5.11 (\pm 0.64) \times 10^{-7}$	0.1247 ± 0.0080
1.58×10^{-5}	$-1.00 (\pm 0.18) \times 10^{-6}$	0.1065 ± 0.0064
3.20×10^{-5}	$-2.72 (\pm 0.38) \times 10^{-6}$	0.1444 ± 0.0060

^a Initial rates are the slopes of plots of $[\text{HCA}]$ versus time using data for the first half-life only. These plots were approximately linear over one half-life. Uncertainties represent 95% confidence intervals. ^b See footnote c in Table 1.

by placing in a serum bottle (no more than half-full), sparging with N₂, crimp-sealing as described above, and then autoclaving at 121 °C for 20 min. All other glassware and items (such as polypropylene pipet tips or Teflon-coated septa) used in longer-term experiments were autoclaved under the same conditions.

Analysis of HCA, PCE, and pentachloroethane (PCA) in aqueous samples was done as follows. At appropriate time points, ampules were centrifuged at approximately 1000 rpm and broken open, and 75 μ L of the supernatant was removed with a microsyringe and extracted with 1.5 mL of 2,2,4-trimethylpentane containing 6 μ M 1,3,5-trichlorobenzene as an internal standard. Extracted samples were analyzed on a Hewlett-Packard (HP) (Palo Alto, CA) 6890 GC with a J&W Scientific (Folsom, CA) DB-5 column (30 m \times 0.53 mm i.d. \times 1.5 μ m film thickness) and an electron capture detector (ECD). Injector temperature was 250 °C and detector temperature was 275 °C. Oven temperature was continuously ramped from 75 to 250 °C at a rate of 15 °C/min and then was isothermal at 250 °C for 1 min. Concentrations of HCA, PCA, and PCE were quantified by comparison of GC peak areas to a five-point standard curve.

Selected aqueous samples were also analyzed on a HP 5890 GC with a HP 19395 headspace autosampler as described below to identify dechlorination products with fewer chlorine atoms than PCE. Carrier gas flow from the headspace autosampler was through a J&W Scientific DB-624 column (30 m \times 0.53 mm i.d. \times 3 μ m film thickness) and then was split via a valve to a second DB-624 column in parallel with a J&W Scientific GS-Q column (30 m \times 0.5 mm i.d.) leading to an ECD and a flame ionization detector (FID), respectively. Injector temperature was 140 °C, and detector temperatures were 250 °C (FID) and 300 °C (ECD). Oven temperature was initially isothermal at 40 °C for 10 min, then ramped at 5 °C/min to 90 °C, then ramped at 20 °C/min to 225 °C, and then isothermal at 225 °C for 2 min. Standards of relevant organic compounds with retention times intermediate between and including trichloroethylene and ethylene, with the important exception of vinyl chloride, have been detected using this method. If present, vinyl chloride would not have been detected due to coelution with the large methanol peak from the HCA spiking solution that was present in every sample.

Aqueous concentrations of pyridine and 2,2'-bipyridine were determined by analysis on a HP 1050 high-performance liquid chromatograph with an Alltech (Deerfield, IL) Altima C₁₈ column (pyridine) or Lichrosorb diol 5U column (2,2'-bipyridine) and a Waters Associates (Milford, MA) model 440 absorbance detector set at 254 nm. The eluent was 65% acetonitrile/35% 0.05 M KH₂PO₄ (pyridine) or 50% methanol/50% 0.025 M K₂HPO₄ (2,2'-bipyridine). Concentrations were quantified by comparison of peak areas to a five-point standard curve.

pH Control. Because initial experimental results (Table 1) showed a strong influence of pH on reaction rate,

TABLE 3. Observed First-Order Rate Constants as a Function of Ionic Strength and Solution Composition for 10 g/L FeS, 0.1 M Tris Buffer, pH 8.3, and an Initial Aqueous HCA Concentration of Approximately 16 μ M

ionic strength (M)	solution amendments ^a	k_{obs} (h^{-1}) ^b	comparison to baseline rate ^c
0.1 ^d	none ^d	0.1065 ± 0.0064^d	not applicable
0.06	none	0.1186 ± 0.0079	
0.5	none	0.136 ± 0.014	+
0.1	1×10^{-3} M NaHS	0.1152 ± 0.0079	
0.1	1×10^{-3} M $\text{FeCl}_2 \cdot 4\text{H}_2\text{O}$	0.1308 ± 0.0038	+
0.1	0.1 M NO_3^- (as HNO_3 and NaNO_3)	0.1039 ± 0.0060	
0.1	3.3×10^{-2} M SO_4^{2-} (as H_2SO_4 and Na_2SO_4)	0.1128 ± 0.0068	
0.1	1×10^{-3} M $\text{CaCl}_2 \cdot 2\text{H}_2\text{O}$	0.0922 ± 0.0091	
0.1	1×10^{-3} M $\text{MnCl}_2 \cdot 4\text{H}_2\text{O}$	0.0946 ± 0.0075	
0.1	1×10^{-3} M EDTA (as $\text{Na}_2\text{H}_2\text{EDTA}$ and Na_4EDTA)	0.143 ± 0.016	+
0.1	1×10^{-3} M sodium oxalate	0.098 ± 0.010	
0.1	1×10^{-3} M sodium succinate	0.099 ± 0.010	
0.1	1×10^{-3} M hydroquinone	0.091 ± 0.012	
0.1	2.5×10^{-4} M pyridine	0.1180 ± 0.0094	
0.1	1×10^{-5} M 2,2'-bipyridine	0.109 ± 0.012	
0.1	3.2×10^{-5} M 2,2'-bipyridine	0.138 ± 0.021	+
0.1	6.6×10^{-5} M 2,2'-bipyridine	0.192 ± 0.036	+
0.1	1×10^{-4} M 2,2'-bipyridine	0.337 ± 0.038	+
0.1	5×10^{-4} M 2,2'-bipyridine	0.810 ± 0.304	+
0.1	1×10^{-3} M 2,2'-bipyridine	1.20 ± 0.39	+
0.1	1×10^{-3} M 1,10-phenanthroline	2.5 ± 1.0	+
0.1	1×10^{-3} M 4,4'-bipyridine	0.090 ± 0.013	
0.1	1×10^{-3} M ethylenediamine	0.098 ± 0.011	
0.1	1×10^{-3} M cysteine	0.0545 ± 0.0069	-
0.1	1×10^{-3} M methionine	0.089 ± 0.011	-

^a None means the solution contained only NaCl, HCl, and Tris buffer. ^b See footnote c in Table 1. ^c + means significantly greater than the baseline rate constant, and - means significantly less than the baseline rate constant. The baseline conditions and rate constant are given in the first line of this table. ^d These are the baseline conditions and rate constant to which others are compared in the text discussion. Data from this experiment are illustrated in Figure 1.

subsequent experiments (Tables 2 and 3) were done in solutions buffered at pH 8.3 by 0.05 M each of tris-(hydroxymethyl)aminomethane (Tris) and Tris-HCl (this combined pH buffer is referred to below as Tris buffer). In order for this concentration of Tris buffer (0.1 M total) to adequately control solution pH, the FeS concentration could be no higher than 10 g/L. Addition of 0.01 N acid in addition to 0.1 M Tris buffer was required to achieve pH 8.3 for 10 g/L FeS. Unless otherwise noted in Table 3, acid was added as HCl. In the absence of FeS, 0.1 M Tris buffer did not cause reductive dechlorination of HCA over a period of several months.

Results and Discussion

Reaction Products and Kinetics. The only product of HCA reductive dechlorination detected in significant quantities under any experimental conditions was PCE, which is the product of HCA dichloroelimination. In many cases, PCA was detected at initial time points in quantities estimated to be below 0.2 μ M (approximately 1% of the original HCA concentration). PCA concentration reached a maximum at early time points and then subsequently decreased below detection limits, indicating that PCA was an intermediate in the transformation of HCA to PCE. TCE, *cis*-1,2-dichloroethylene (*cis*-1,2-DCE), and acetylene were detected over longer time periods, indicating that they were subsequent reaction products. TCE and *cis*-1,2-DCE reached concentrations no greater than approximately 0.6 and 0.2 μ M, respectively, after approximately 2.5 months. Acetylene was not quantified but was estimated to be present at micromolar concentrations after 2.5 months.

The results of a series of experiments done at different FeS concentrations and at pH values of 7.7–7.8 (Table 1) indicate that the rate of HCA reductive dechlorination by FeS was proportional to FeS concentration for the range of concentrations investigated here. Reductive dechlorination of HCA by FeS was shown to be first-order with respect to

HCA concentration by analysis of the data shown in Table 2. This table shows the results of a series of experiments in which the initial rate of HCA disappearance was measured for a range of initial HCA concentrations at a single FeS concentration (10 g/L) and pH value (8.3). Using the initial-rate method (23, 24), the reaction order with respect to HCA was determined to be 0.9 ± 0.4 or approximately 1. (The uncertainty in this value is the 95% confidence interval.) The good fit of these and other experimental data to a first-order rate model and the fairly good agreement among the observed first-order rate constants for experiments having a range of initial HCA concentrations (Table 2) are also consistent with a reaction that is first-order with respect to HCA concentration over the range of concentrations studied here.

Figure 1 shows a typical plot of HCA and PCE concentrations versus time in the presence of 10 g/L FeS. Error bars in this and other figures are 95% confidence intervals. The solid line for HCA in Figure 1 represents the best fit of the experimental data to a first-order rate law. Observed first-order rate constants, valid for a given FeS concentration, are reported in Tables 1–3. To obtain the solid line for PCE in Figure 1, it was first assumed that the mass of PCE at any time (PCE_t) was given by

$$\text{PCE}_t = \text{HCA}_0 - \text{HCA}_t + \text{PCE}_0 \quad (1)$$

where HCA_0 , HCA_t , and PCE_0 are the masses of these compounds at times 0 and t . (PCE was present in the HCA used in these experiments as a minor impurity, accounting for the PCE_0 term in eq 1.) Each term in eq 1 was assumed to be the sum of two components: headspace mass and aqueous mass. Utilizing measured aqueous and headspace volumes and dimensionless Henry's constants of 0.41 for HCA (25) and an average value of 0.785 for PCE (25–28), eq 1 was rewritten as a function of the aqueous concentration of PCE at any time, $[\text{PCE}]_{\text{aq},t}$, and plotted as the solid line for PCE in Figure 1. The fairly good agreement between this

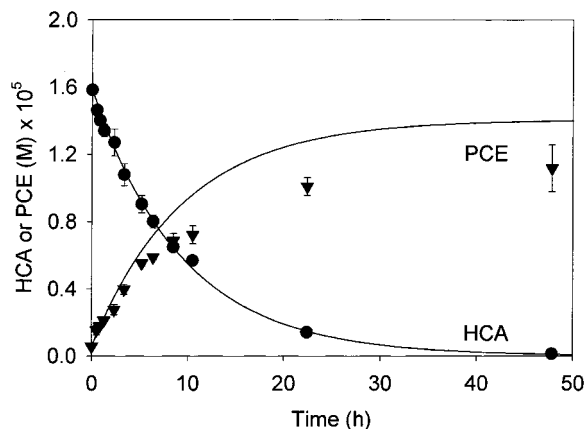


FIGURE 1. HCA and PCE versus time; 10 g/L FeS, 0.1 M Tris buffer, pH 8.3; $I = 0.1$ M. The solid line for HCA represents the best fit of experimental data to a first-order rate law, i.e., $[HCA] = [HCA]_0 e^{-kt}$. The solid line for PCE represents the concentrations that would result if the PCE resulting from HCA degradation partitioned between the sample aqueous and gas phases according to Henry's law.

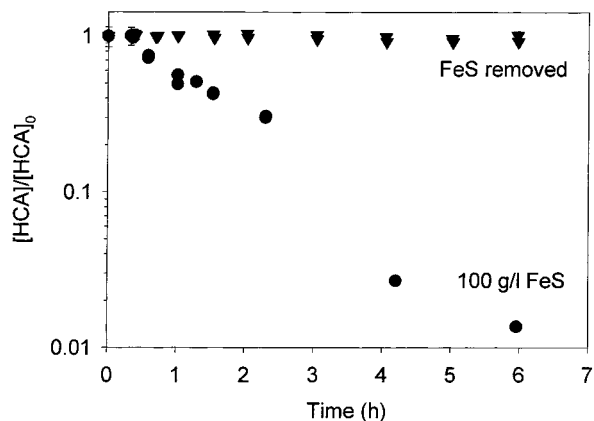


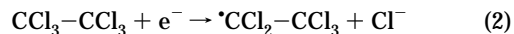
FIGURE 2. $[HCA]/[HCA]_0$ versus time; pH 7.8, $I = 0.1$ M, initial aqueous HCA concentration: approximately $16 \mu\text{M}$.

line and measured concentrations of PCE versus time illustrates that losses to the sample headspace account for most of the incomplete PCE recovery from HCA. It should be noted that these computations were used only to illustrate PCE recovery in Figure 1 and not in quantitative analysis of rate data described later in this paper.

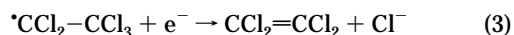
To confirm that the reaction was dependent upon FeS surface species, including both structural and adsorbed ferrous and sulfide, and not dissolved aqueous species in equilibrium with FeS, an experiment was conducted in which two 100 g/l FeS slurries were prepared identically at pH 7.8 and equilibrated overnight. Prior to spiking with HCA, the solid phase was removed from one slurry by centrifugation. The results are shown in Figure 2 on a semilogarithmic scale to further illustrate agreement of the kinetic data to a rate law that is first-order with respect to HCA. Figure 2 also shows that the dechlorination rate in the absence of FeS was not significant as compared to the rate when FeS was present, indicating that FeS surface species are responsible for the relatively rapid reductive dechlorination of HCA observed in the experimental systems described here. Analysis of samples in which FeS had been removed by centrifugation after longer time periods indicated that, in the absence of FeS, complete transformation of HCA to PCE took place over the course of months rather than hours. The difference in the reductive dechlorination rate for dissolved ferrous and sulfide species versus FeS could be due to one or more of several factors, including a more favorable free energy for oxidation of FeS

versus $\text{Fe}^{2+}(\text{aq})$ or $\text{HS}^-(\text{aq})$, the ability of solid surfaces to increase reaction rates by lowering activation energies, and the electronic properties of the bulk mineral.

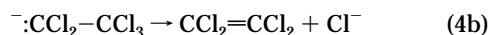
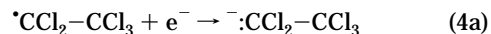
Dichloroelimination of HCA to PCE as in Figure 1 represents an overall two-electron reduction since the formal oxidation state of each carbon atom in HCA is +III while in PCE it is +II. There are several pathways by which such a reaction might take place. First, the reaction might proceed by two successive one-electron transfers, typical of alkyl halide reduction by transition metals (29), with the rate-limiting step being concurrent electron transfer and carbon-chlorine bond cleavage (30), in this case forming the pentachloroethyl radical:



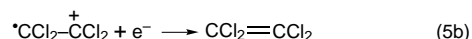
The most likely pathways for subsequent radical decomposition include (31) a second concurrent electron transfer and carbon-chlorine bond cleavage reaction



slow electron transfer followed by fast carbon-chlorine bond cleavage



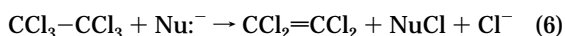
or fast carbon-chlorine bond cleavage followed by slow electron transfer



The detection of the HCA hydrogenolysis product PCA as an intermediate is consistent with any of these pathways, since it could form by abstraction of a hydrogen atom (possibly from methanol or the FeS solid) by the pentachloroethyl radical produced in reaction 2 or by protonation of the pentachloroethyl anion produced in reaction 4a. Radioisotope studies have shown that hydrogenolysis products of other chlorinated organics are formed both by hydrogen atom abstraction by radical intermediates (32) and by protonation of anion intermediates (33), so it is not possible to distinguish which is the most likely among reactions 2–5 on the basis of the experimental evidence described here. However, it has been proposed that reaction 3 is a more probable radical decomposition path in dihaloelimination than 4a,b or 5a,b, at least for vicinal dibromoalkanes, due to the strong driving force for double bond formation (31).

According to the terminology of Lexa et al. (31), reactions 2–5 are outer-sphere electron-transfer steps with respect to the electron donor, since no bonds to the donor are formed or broken concurrent with electron transfer and the transition state does not involve bonding interactions between donor and acceptor. This is in contrast to an inner-sphere pathway in which electron transfer takes place concurrent with bond breaking or formation and in which bonding interactions stabilize the transition state (31). Nucleophiles such as sulfides and polysulfides have been shown to cause vicinal dihaloelimination reactions such as the dichloroelimination of HCA to PCE (34–36) by a two-electron reduction reaction (29), which, by the same terminology (31), can be classified as inner-sphere with respect to the electron donor. Since the FeS surface may contain nucleophilic S(–II) functional groups, this is another plausible pathway for the observed dichloroelimination of HCA to PCE. Such a reaction could occur in a single bimolecular step (E2 elimination), which

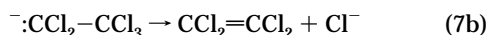
does not allow for production of PCA as an intermediate



("Nu:" means nucleophile) or via pathways that involve separate unimolecular and bimolecular steps. E1 elimination, with chloride ion loss as the rate-limiting unimolecular step, is not in agreement with the observed dependence of the reaction rate on the concentrations of both HCA and FeS. Another possibility is a mechanism analogous to E1cb (unimolecular elimination of the conjugate base), in which the rate-limiting step is bimolecular chloronium ion removal, forming a carbanion



followed by fast unimolecular chloride ion expulsion to form PCE.



Reactions 7a and 7b are shown here since protonation of the carbanion intermediate produced in reaction 7a is another conceivable pathway for PCA production (37). However, elimination via carbanions as in reactions 7a and 7b is reportedly seldom observed (38). In addition, the most likely pathway for base-catalyzed elimination of HCA to PCA was found to be E2 and not E1cb (37), and dichloroelimination of HCA to PCE via E1cb elimination seems even less likely since it involves initial expulsion of a chloronium ion rather than a proton. Taken together, the observed dependence of the reaction rate on both HCA and FeS concentrations and the detection of PCA as a reaction intermediate, which could not be produced by E2 elimination and is not likely to be produced by E1cb, support a HCA dichloroelimination pathway involving two successive one-electron transfers as in reactions 2–5. The electrons involved in these reactions may come from delocalized orbitals within the mackinawite layer structure that arise from bonding interactions between $d_{x^2-y^2}$ orbitals of closely spaced iron atoms (39). This orbital picture is consistent with band-structure calculations which indicate that mackinawite is a metallic conductor with a conduction band of mainly d character (40).

Influence of pH. Increasing solution pH between 7.1 and 9.5 caused a significant increase in the rate of reductive dechlorination of HCA by FeS for a series of experiments done with 100 g/L FeS (Table 1). To interpret this result, it was assumed that the hydrated FeS surface consists of hydroxide functional groups similar to those of transition metal oxides as well as bisulfide functional groups unique to sulfides. These functional groups are believed to form on the surfaces of lead and zinc sulfides in aqueous solution from hydrolysis of partially uncoordinated surface metal and sulfur atoms, which then undergo protonation and deprotonation reactions as solution pH changes (41). A schematic diagram of such plausible hydrolysis and acid/base reactions for the FeS surface is shown in Figure 3. It is hypothesized that a pH-dependent equilibrium between the protonated and deprotonated forms of similar FeS surface species, with the deprotonated species having greater reactivity, is responsible for the pH dependence of the rate of reductive dechlorination of HCA by FeS.

On the basis of the relative acidities of H_2O and H_2S , Sun et al. (41) have proposed that, below the pH_{pzc} (the pH at which the net surface charge is zero) of lead and zinc sulfides, the most important surface acid/base equilibrium is between $\equiv\text{MeOH}_2^+$ and $\equiv\text{MeOH}$, while above the pH_{pzc} the most important acid/base equilibrium is between $\equiv\text{MeSH}$ and $\equiv\text{MeS}^-$, where Me is the metal and \equiv indicates the bulk mineral, and where each $\equiv\text{Me}$ is bonded to one or more bulk

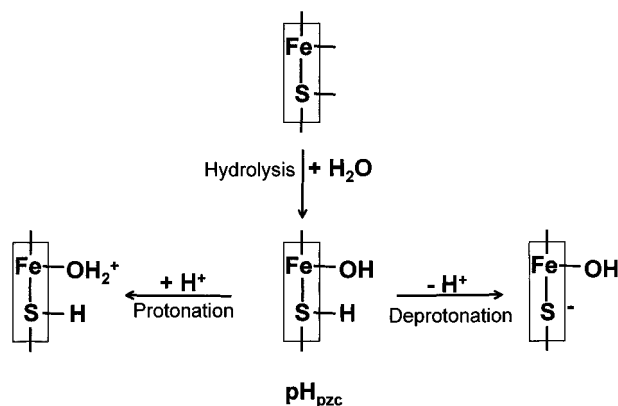


FIGURE 3. FeS surface hydrolysis and acid/base reactions (based on ref 41). Shaded boxes represent the FeS surface.

sulfur atoms. On this basis and assuming that the pH_{pzc} for FeS corresponds to its pH of minimum solubility [approximately 10.1, based on chemical equilibrium calculations using MINEQL+ (42)], it is hypothesized that the most significant change in FeS surface acid/base speciation in the pH range that was investigated (7.1–9.5) results from the reaction



for which there is a characteristic acid dissociation constant (K_a). The K_a discussed here is a conditional equilibrium constant since it is written in terms of concentrations and not activities without consideration of surface charge effects. The observation that FeS slurries became increasingly difficult to centrifuge as the pH decreased from 9.5 to 7.1 is consistent with a pH-dependent equilibrium between a neutral and a positively charged surface species, which would result in increased interparticle repulsion and decreased flocculation with decreasing pH.

Next, experimental results were interpreted using a methodology similar to that used by Millero (43) in explaining the pH dependence of O_2 reduction by aqueous Fe(II). Assuming that the two surface species $\equiv\text{FeOH}_2^+$ and $\equiv\text{FeOH}$ have different reactivities with respect to reductive dechlorination and assuming that the sum of the concentrations of these two species equals the total reactive surface iron ($[\equiv\text{Fe}]_T$), i.e.

$$[\equiv\text{Fe}]_T = [\equiv\text{FeOH}_2^+] + [\equiv\text{FeOH}] \quad (9)$$

yields a rate law of the form

$$-\frac{d[\text{HCA}]}{dt} = k_0[\text{HCA}][\equiv\text{FeOH}_2^+] + k_1[\text{HCA}][\equiv\text{FeOH}] = k_{\text{tot}}[\text{HCA}][\equiv\text{Fe}]_T \quad (10)$$

where k_0 and k_1 are the rate constants associated with $[\equiv\text{FeOH}_2^+]$ and $[\equiv\text{FeOH}]$, respectively, and k_{tot} is the total rate constant. By defining the ionization fractions α_0 and α_1 as

$$\alpha_0 = \frac{[\equiv\text{FeOH}_2^+]}{[\equiv\text{Fe}]_T}$$

and

$$\alpha_1 = \frac{[\equiv\text{FeOH}]}{[\equiv\text{Fe}]_T} \quad (11)$$

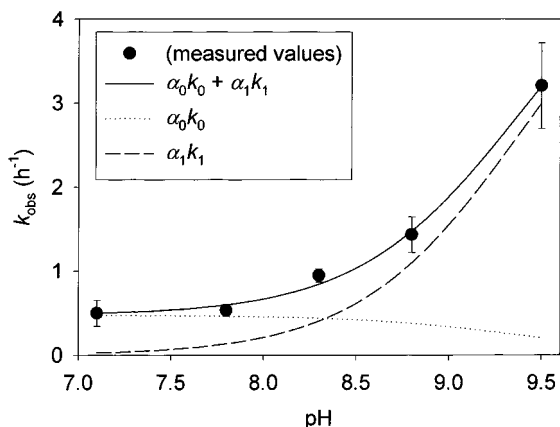


FIGURE 4. Observed first-order rate constants versus pH; $I = 0.1$ M, 100 g/L FeS, initial aqueous HCA concentration: approximately 16 μ M.

eq 10 can be simplified to

$$k_{\text{tot}} = \alpha_0 k_0 + \alpha_1 k_1 \quad (12)$$

By combining eqs 8, 9, and 11, α_0 and α_1 (and therefore eq 12) can be shown to be functions of K_a and pH.

Experimentally measured k_{tot} values for HCA reductive dechlorination by 100 g/L FeS as a function of pH are reported in Table 1. For consistency with the other rate constants reported here, the "tot" subscript is omitted in Table 1. These measured rate constants were fit to eq 12 using a statistical program with three adjustable parameters: K_a , k_0 , and k_1 . Best fit of the data was obtained for $K_a = 10^{-9.4}$ M, $k_0 = 0.47$ h^{-1} , and $k_1 = 5.3$ h^{-1} ($r^2 = 0.997$). This value of K_a is in theory independent of FeS concentration, but the values of k_0 and k_1 are unique to 100 g/L FeS. The large difference in magnitude between k_0 and k_1 , and thus the large difference in reactivities between FeOH_2^+ and FeOH , can be explained by assuming that the driving force for electron donation by surface Fe(II) species is increased by the larger electron density on the more deprotonated ligand (44). Experimental values of k_{obs} fit with model parameters are shown in Figure 4. Figure 4 also shows the individual contributions of both $\alpha_0 k_0$ and $\alpha_1 k_1$ to the total rate constant, illustrating that increased concentration of the more deprotonated species is the principal cause of the rate increase at higher pH values.

A similar pH dependence has been observed in the reduction of nitroaromatics by both Fe(II) adsorbed to magnetite (45) and by an iron porphyrin (46). For Fe(II) adsorbed to magnetite, the pH dependence was explained in part by the formation of Fe(II) surface complexes with different reactivities as a function of pH. In the case of the Fe(II) porphyrin, increased pH was thought to result in increased stabilization of the Fe(III) versus the Fe(II) porphyrin, increasing the driving force for electron transfer as a porphyrin axial ligand became more deprotonated.

Despite good agreement between experiment and model in the pH range of 7.1–9.5 as well as agreement with the trends observed in other experimental systems involving Fe(II), direct evidence for the existence and reactivities of the Fe surface species postulated above has not been obtained. Consequently, eq 12 should be considered an operational or empirical rate expression that could apply equally well to other surface acid/base pairs, for instance FeSH_2^+ and FeSH or FeSH and FeS^- , or even a combination of species such as these. In addition, it is likely that outside the pH range of 7.1–9.5 additional surface acid/base equilibria are important and should be considered. However, the following indirect evidence supports the existence of the

TABLE 4. Equilibrium Constants for Complex Formation Reactions; $I = 0$ M, $T = 25$ $^\circ\text{C}$

L	$\log \beta_1^a$ (ref)
NO_3^-	0.2 ^b
Cl^-	0.9 (42)
SO_4^{2-}	2.2 (52)
EDTA^{4-}	16.1 (52)
oxalate	4.2 (53)
succinate	not available
hydroquinone	not available
pyridine	0.6 (53)
2,2'-bipyridine	4.20 (53)
1,10-phenanthroline	5.85 (53)
4,4'-bipyridine	not available
ethylenediamine	4.3 (52)
cysteine	5.1 ^c (54)
methionine	3.24 ^d (53)

^a β_1 is the equilibrium constant for the reaction $\text{Fe}^{2+} + \text{L}^{x-} = \text{ML}^{2-x}$. Certain values of β_1 were adjusted to zero ionic strength using the Davies equation. ^b Value estimated from β_1 values for Mn^{2+} and Co^{2+} from ref 53. ^c Conditional equilibrium constant measured at pH 7–8. ^d β_1 for 20 $^\circ\text{C}$.

reactive surface Fe(II) species proposed above for the range of pH values studied here. First, the addition of 1 mM Fe^{2+} to a 10 g/L FeS slurry at pH 8.3 immediately before spiking with HCA caused a slight increase in the HCA dechlorination rate, while the addition of 1 mM HS^- did not significantly influence the rate (Table 3), supporting the idea that an equilibrium between surface iron species and not surface sulfur species may be responsible for the pH-dependent rate behavior. Second, others have performed X-ray photoelectron spectroscopy of the native surface of FeS (troilite) shown to cause dechlorination of TCE and detected no sulfide, only oxidized forms of sulfur, from which it was concluded that surface-bound iron species rather than sulfide species were mediating the observed dechlorination reaction (17).

Influence of Ionic and Organic Solution Composition.

This section discusses experiments in which various ionic and organic compounds representative of species found in natural waters were added to the FeS slurry prior to spiking with HCA. The purpose of these experiments was to assess the influence of relevant species with different affinities for Fe(II) and S(–II) surface functional groups on the dechlorination reaction rate and thereby gain further information about the FeS reactive species involved in HCA reductive dechlorination as well as the likely progress of dechlorination reactions in natural systems. Observed first-order rate constants for these experiments are reported in Table 3. The first entry in this table represents the baseline rate constant and experimental conditions (i.e., no solution amendments except 0.1 M Tris buffer and NaCl to establish ionic strength) to which the other entries are compared. Data for this experiment are illustrated in Figure 1. When available, equilibrium constants for formation of complexes between ionic and organic compounds and Fe^{2+} are given in Table 4 as an estimate of the relative affinities of these compounds for surface Fe(II) functional groups.

Varying the ionic strength from 0.06 to 0.1 M by varying NaCl concentration had no significant effect on the rate of HCA reductive dechlorination by FeS, but a slight increase in rate was observed when ionic strength was increased from 0.1 to 0.5 M. There are numerous ways in which ionic strength might affect the HCA reductive dechlorination rate, including changes in the conditional equilibrium constants discussed in the last section or effects on the available FeS surface area through increased or decreased coagulation and flocculation. However, the absence of a consistent correlation between reaction rate and ionic strength for the range $I = 0.06$ –0.5 M does not allow conclusive interpretation of these data.

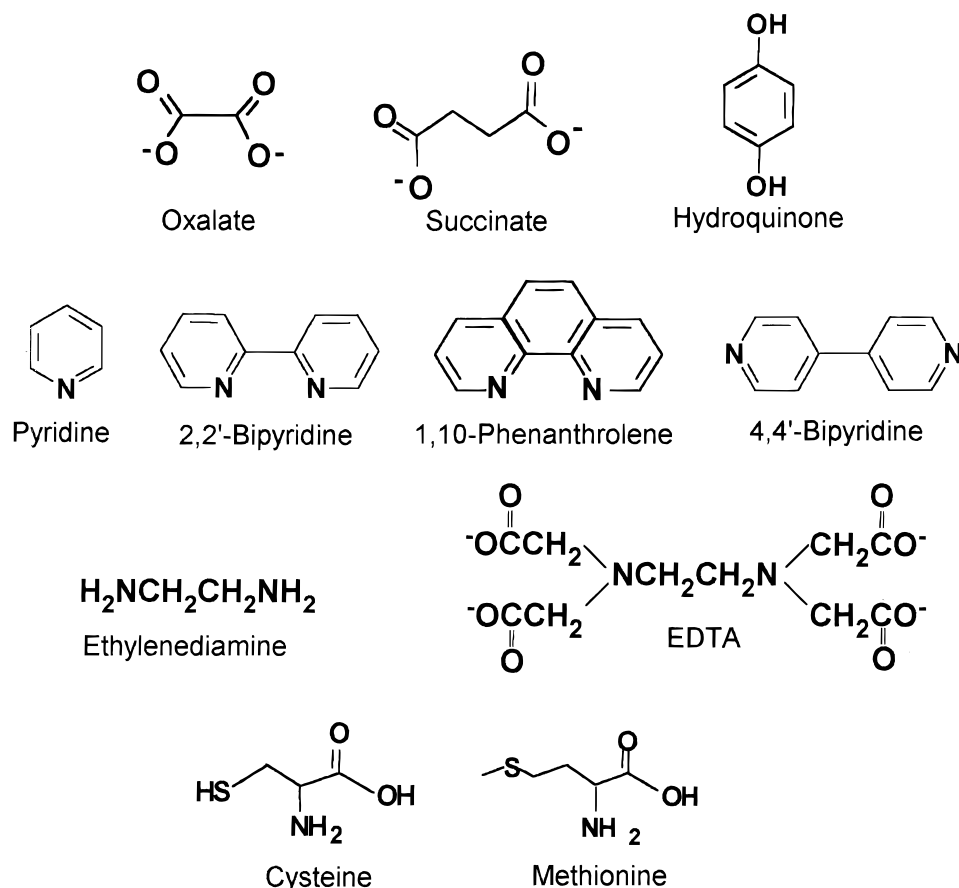


FIGURE 5. Organic amendments to FeS experimental systems.

Inorganic solution composition was varied by establishing an ionic strength of 0.1 M through the addition of the sodium salts of three different anions: NO_3^- , Cl^- , and SO_4^{2-} . These anions vary in their free energies of complex formation with Fe^{2+} (with the free energy of complex formation becoming more favorable in the order that the anions are listed above). It was hypothesized that the FeS aqueous solution containing the anions with the greatest affinity for Fe^{2+} would have the slowest reductive dechlorination rate due to adsorption to Fe(II) surface sites. However, no significant effect of anion composition on reductive dechlorination rates for these three experimental systems was observed (Table 3).

Numerous organic amendments containing functional groups representative of natural organic matter (Figure 5) and with different affinities for Fe(II) (Table 4) were also added to the FeS aqueous slurry prior to spiking with HCA. With the exceptions noted in Table 3, these compounds were added at millimolar or higher concentrations, which were expected to be sufficient for at least monolayer adsorption based on measured FeS specific surface area. Measurements of the adsorption of pyridine to the FeS surface indicated that the maximum adsorption density was approximately 0.01 mg/g or about one pyridine molecule per every 0.6 nm² (based on BET surface area) and that this maximum adsorption density occurred at or below a total pyridine concentration of 1×10^{-4} M for 10 g/L FeS at pH 8.3. Although this adsorption density is less than monolayer coverage, it is still significant and provides a reference to which other organic compounds in Table 3 can be compared based on their equilibrium constants for complex formation with Fe^{2+} .

Oxalate, succinate, and hydroquinone, which contain phenolic and carboxylic functional groups, had no significant effect on the HCA dechlorination rate. Although the driving

forces for succinate and hydroquinone adsorption to the FeS surface are not known, oxalate has a relatively large equilibrium constant for complex formation with Fe^{2+} as compared to pyridine (Table 4), indicating that significant adsorption of oxalate to the FeS surface is likely. Nevertheless, no significant effect on the reaction rate was observed when oxalate was present. This result along with the fact that anion composition did not significantly influence reaction rates is consistent with an electron-transfer mechanism that is outer sphere with respect to the electron donor as in reactions 2–5. An inner-sphere pathway would likely be very sensitive to the presence of coordinating ligands (47) since close interaction between FeS surface functional groups and HCA would be required for electron transfer to take place. An outer-sphere electron-transfer mechanism such as reactions 2–5 is also consistent with detection of PCA as a reaction intermediate.

Addition of Ca^{2+} or Mn^{2+} as their chloride salts to FeS slurries also did not have a significant impact on the reaction rate (Table 3), despite the fact that Mn^{2+} has been shown to adsorb to a significant extent to mackinawite at pH 7 (48). The lack of any effect of Mn^{2+} on the reaction rate is further evidence that HCA transformation to PCE takes place via successive one-electron transfers as in reactions 2–5 rather than by an inner-sphere elimination pathway mediated by surface sulfide functional groups as in reactions 6–7, since coordination of these sulfide groups by Mn^{2+} would likely affect the rate of such a reaction.

Certain aliphatic amines and aromatic nitrogen heterocyclic compounds significantly affected the rate of HCA reductive dechlorination by FeS. For example, the addition of 1 mM 2,2'-bipyridine to FeS slurries caused a 10-fold increase in the rate of HCA reductive dechlorination (Table

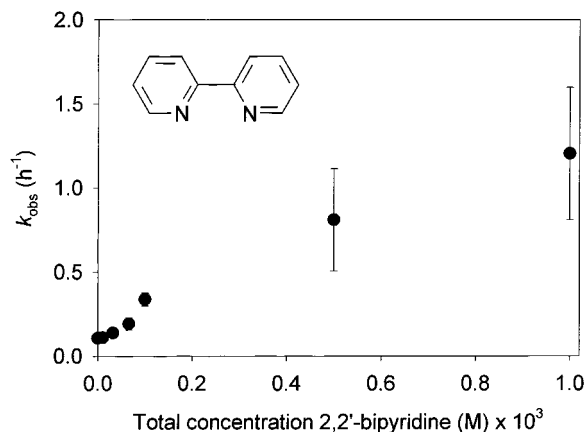


FIGURE 6. Observed first-order rate constants versus total concentration 2,2'-bipyridine; 10 g/L FeS, 0.1 M Tris buffer, pH 8.3; $I = 0.1$ M, initial aqueous HCA concentration: approximately 16 μ M.

3). Observed first-order rate constants versus total 2,2'-bipyridine concentration for 10 g/L FeS at pH 8.3 are plotted in Figure 6. Concentrations of 2,2'-bipyridine measured in the supernatant of centrifuged FeS slurries were below quantitative detection limits (approximately 10^{-6} M) over the total 2,2'-bipyridine concentration range shown in Figure 6, indicating that the majority of the 2,2'-bipyridine in these experiments was associated with the mineral surface. This indicates that the rate increase is likely due to participation of a surface Fe(II)-2,2'-bipyridine complex in the electron-transfer reaction. In addition, there was no significant HCA dechlorination in the time scale of interest in solutions of Fe(II)(aq) and 2,2'-bipyridine when FeS was not present (data not shown), providing further evidence that the FeS surface is involved in the rapid reductive dechlorination of HCA in the presence of 2,2'-bipyridine. Addition of 1,10-phenanthroline, which has a structure similar to 2,2'-bipyridine, to the reaction mixture also dramatically enhanced the reaction rate (Table 3). However, while ethylenediaminetetraacetic acid (EDTA) caused a small increase in the reaction rate, 4,4'-bipyridine, pyridine, and ethylenediamine had no significant effect.

Thus, the only compounds in this group found to significantly affect the rate of HCA reductive dechlorination were those with a bidentate chelating functional group arising from lone pairs on each of two nitrogen atoms bound to adjacent carbon atoms, i.e., 2,2'-bipyridine, 1,10-phenanthroline, and EDTA. The presence of this functional group likely increased the driving force for adsorption of these compounds to the mineral surface. Compounds that were monodentate or bridging ligands (i.e., pyridine or 4,4'-bipyridine, respectively) had no significant effect on the reaction rate. Furthermore, of the bidentate chelating ligands that caused a rate increase, those with aromatic functionality affected the rate the most. This is evident by the fact that 2,2'-bipyridine and 1,10-phenanthroline dramatically increased the reaction rate, while EDTA caused only a slight rate increase and ethylenediamine had no significant effect. 4,4'-Bipyridine, which possesses the aromatic functional group of 2,2'-bipyridine and 1,10-phenanthroline but not the bidentate chelating functional group, had no significant effect on the rate. Thus, both the bidentate chelating functionality and the aromatic functionality appear to be required for the rate increase.

It is likely that polynuclear aromatic functional groups in 2,2'-bipyridine and 1,10-phenanthroline increased the HCA dechlorination rate by facilitating electron transfer in the FeS/HCA system. Electrochemical reduction studies of the Fe(II)/2,2'-bipyridine complex indicate that electrons gained

when this compound is reduced reside mainly in molecular π^* orbitals (49). Because these orbitals are delocalized over the entire molecule, electron transfer from these orbitals requires smaller changes in bond lengths and molecular geometry than would be the case for orbitals localized on the metal atom, thus lowering the activation energy for electron transfer (50). A similar rationale has been used by others to explain the greater rate of electron exchange between the Fe(II) and Fe(III) complexes of 1,10-phenanthroline versus other Fe(II)/Fe(III) exchanges (51). Assuming similar behavior in the presence of FeS, 2,2'-bipyridine and 1,10-phenanthroline might facilitate electron transfer in the FeS/HCA system by allowing electron transfer from the bulk solid phase to HCA via delocalized π^* molecular orbitals associated with a surface complex.

Since numerous natural products and biochemicals, including porphine derivatives such as transition metal coenzymes and compounds containing purine derivatives such as nucleic acids, contain both the multidentate chelating capacity of a compound such as 2,2'-bipyridine and its polynuclear aromatic functionality, the presence of these compounds in natural systems may strongly influence the rates of intrinsic abiotic reductive dechlorination by FeS.

The addition of 1 mM cysteine, a thiol-containing amino acid, to the FeS reaction mixture reduced the rate of reductive dechlorination of HCA by almost one-half, and the addition of 1 mM methionine, an alkylthio amino acid, very slightly depressed the rate (Table 3). This rate reduction may be due to adsorption of cysteine or methionine to surface iron atoms in competition with HS^- or OH^- , causing an energetic or steric barrier to electron transfer. Adsorption to surface iron functional groups would be facilitated by the large driving force for iron-sulfide complex formation. This explanation for the slowed rate in the presence of cysteine is consistent with the model of reactive Fe(II) surface functional groups discussed earlier and with the observation that the addition of Fe^{2+} to FeS slurries increased the reaction rate. The difference in the effects of cysteine and methionine on the reaction rate might be explained by the difference in the equilibrium constants for complex formation between these amino acids and Fe^{2+} (Table 4). Depending on structure and function, other thiol- and sulfide-containing natural products may also affect the rates of reductive dechlorination of chlorinated pollutants in aquatic systems.

Environmental Significance. FeS was shown to dechlorinate HCA relatively rapidly, with half-lives on the order of hours to days. The reaction was relatively insensitive to the presence of numerous ionic and organic species common in natural waters, and in some cases showed a significant increase in reaction rate when certain multidentate aromatic nitrogen heterocyclic compounds were present. The compounds shown to decrease the reaction rate, cysteine and methionine, caused less than a 50% rate decrease, even when present at concentrations much higher than they are likely to be present in natural waters. The insensitivity of this reaction to numerous ionic and organic amendments suggests that FeS may retain its reactivity even in rather diverse solution environments. For this reason, FeS may prove to be a useful alternative or addition to zero-valent iron for some in-situ reactive barrier applications, particularly since FeS (troilite) has been shown (19) to react more than an order of magnitude faster than granular iron in TCE dechlorination. However, the effects of weathering under field conditions on the reactivity of the FeS surface have yet to be explored. The results described here also indicate that abiotic dechlorination pathways are likely to be significant in sulfide-rich environments where FeS is produced as a result of microbial activity, in addition to the usually assumed predominant pathways of microbial cometabolic reductive dechlorination.

Acknowledgments

We thank Tom Yavaraski for invaluable assistance in the laboratory and John Gland for helpful discussions. We also thank three anonymous individuals for critical review of the manuscript. Funding for this research was provided by the Great Lakes and Mid-Atlantic Center for Hazardous Substance Research under Grant R-819605 from the Office of Research and Development, U.S. Environmental Protection Agency. Partial funding of the research activities of the center was provided by the State of Michigan Department of Natural Resources. The content of this publication does not necessarily reflect the views of either agency. Funding for this research was also provided by a University of Michigan Spring/Summer Research Grant.

Literature Cited

- (1) U.S. Environmental Protection Agency. *Fed. Regist.* **1985**, *50*, 46880 (Nov 13, 1985).
- (2) Criddle, C. S.; McCarty, P. L.; Elliot, M. C.; Barker, J. F. *J. Contam. Hydrol.* **1986**, *1*, 133–142.
- (3) Jafvert, C. T.; Wolfe, N. L. *Environ. Toxicol. Chem.* **1987**, *6*, 827–837.
- (4) Barcelona, M. J.; Holm, T. R. *Environ. Sci. Technol.* **1991**, *25*, 1565–1572.
- (5) Curtis, G. P. Ph.D. Dissertation, Stanford University, 1991.
- (6) Freney, J. R. *The Encyclopedia of Soil Science, Part 1: Encyclopedia of Earth Sciences*, Vol. XII; Fairbridge, R. W., Finkl, C. W., Jr., Eds.; Dowden, Hutchinson and Ross, Inc.: Stroudsburg, PA, 1979; pp 536–544.
- (7) Rickard, D. T. *Stockholm Contr. Geol.* **1969**, *26*, 49–66.
- (8) Berner, R. A. *J. Geol.* **1964**, *72*, 293–306.
- (9) Doyle, R. W. *Am. J. Sci.* **1968**, *266*, 980–994.
- (10) Davison, W. *Aquat. Sci.* **1991**, *53*, 309–321.
- (11) Roberts, A. L.; Sanborn, P. N.; Gschwend, P. M. *Preprints of Papers Presented at the 199th ACS National Meeting*, April 22–27, 1990, Boston, MA; American Chemical Society: Washington, DC, 1990; Vol. 30 (1), pp 46–49.
- (12) Kriegman-King, M. R.; Reinhard, M. In *Organic Substances and Sediments in Water, Vol. 2, Processes and Analytical*; Baker, R., Ed.; Lewis Publishers: Chelsea, MI, 1991; pp 349–364.
- (13) Doong, R.-A.; Wu, S.-C. *Chemosphere* **1992**, *24*, 1063–1075.
- (14) Kriegman-King, M. R.; Reinhard, M. *Environ. Sci. Technol.* **1994**, *28*, 692–700.
- (15) Harms, S.; Lipczynska-Kochany, E.; Milburn, R.; Sprah, G.; Nadarajah, N. *Preprints of Papers Presented at the 209th ACS National Meeting*, April 2–7, 1995, Anaheim, CA; American Chemical Society: Washington, DC, 1995; Vol. 35 (1), pp 825–828.
- (16) Hassan, S. M.; Wolfe, N. L.; Cippolone, M. G. *Preprints of Papers Presented at the 209th ACS National Meeting*, April 2–7, 1995, Anaheim, CA; American Chemical Society: Washington, DC, 1995; Vol. 35 (1), pp 735–737.
- (17) Sivavec, T. M.; Horney, D. P.; Baghel, S. S. *Emerging Technologies in Hazardous Waste Management VII*; American Chemical Society Special Symposium, September 17–20, 1995, Atlanta, GA; ACS: Washington, DC, 1995; pp 42–45.
- (18) Assaf-Anid, N.; Lin, K.-Y.; Mahony, J. *Preprints of Papers Presented at the 213th ACS National Meeting*, April 13–17, 1997, San Francisco, CA; American Chemical Society: Washington, DC, 1997; Vol. 37 (1), pp 194–195.
- (19) Sivavec, T. M.; Horney, D. P. *Preprints of Papers Presented at the 213th ACS National Meeting*, April 13–17, 1997, San Francisco, CA; American Chemical Society: Washington, DC, 1997; Vol. 37 (1), pp 115–117.
- (20) Rickard, D. T. *Stockholm Contr. Geol.* **1969**, *26*, 67–95.
- (21) Burlinson, N. E.; Lee, L. A.; Rosenblatt, D. H. *Environ. Sci. Technol.* **1982**, *16*, 627–632.
- (22) Barbash, J. E.; Reinhard, M. *Environ. Sci. Technol.* **1989**, *23*, 1349–1358.
- (23) Birk, J. P. *J. Chem. Educ.* **1976**, *53*, 704–707.
- (24) Levine, I. N. *Physical Chemistry*, 3rd ed.; McGraw-Hill: New York, 1988; p 527.
- (25) Patterson, J. W. *Industrial Wastewater Treatment Technology*, 2nd ed.; Butterworths: Boston, 1982; pp 320–322.
- (26) Leighton, D. T., Jr.; Calo, J. M. *J. Chem. Eng. Data* **1981**, *26*, 382–385.
- (27) Mackay, D.; Shiu, W. Y. *J. Phys. Chem. Ref. Data* **1981**, *10*, 1175–1199.
- (28) Gossett, J. M. *Environ. Sci. Technol.* **1987**, *21*, 202–208.
- (29) Baciocchi, E. In *The Chemistry of Halides, Pseudo-Halides and Azides*; Supplement D to the Chemistry of Functional Groups; Patai, S., Rappoport, Z., Eds.; Wiley: New York, 1983; pp 161–201.
- (30) Castro, C. E.; Kray, W. C., Jr. *J. Am. Chem. Soc.* **1963**, *85*, 2768–2773.
- (31) Lexa, D.; Savéant, J.-M.; Schäfer, H. J.; Su, K.-B.; Vering, B.; Wang, D. L. *J. Am. Chem. Soc.* **1990**, *112*, 6162–6177.
- (32) Ahr, H. J.; King, L. J.; Nastainczyk, W.; Ullrich, V. *Biochem. Pharmacol.* **1980**, *29*, 2855–2861.
- (33) Nies, L.; Vogel, T. M. *Appl. Environ. Microbiol.* **1991**, *57*, 2771–2774.
- (34) Ramasamy, K.; Kalyanasundaram, S. L.; Shanmugam, P. *Synthesis* **1978**, 311–312.
- (35) Roberts, A. L. Ph.D. Dissertation, Massachusetts Institute of Technology, 1991.
- (36) Curtis, G. P.; Reinhard, M. *Environ. Sci. Technol.* **1994**, *28*, 2393–2402.
- (37) Roberts, A. L.; Gschwend, P. M. *Environ. Sci. Technol.* **1991**, *25*, 76–86.
- (38) Morrison, R. T.; Boyd, R. N. *Organic Chemistry*, 4th ed.; Allyn and Bacon, Boston, 1983; p 290.
- (39) Kjekshus, A.; Nicholson, D. G.; Mukherjee, A. D. *Acta Chem. Scand.* **1972**, *26*, 1105–1110.
- (40) Welz, D.; Rosenberg, M. J. *Phys. C: Solid State Phys.* **1987**, *20*, 3911–3924.
- (41) Sun, Z.; Forsling, W.; Rönngren, L.; Sjöberg, S. *Int. J. Miner. Process* **1991**, *33*, 83–93.
- (42) Schecher, W. D.; McAvoy, D. C. *MINEQL+, A Chemical Equilibrium Program for Personal Computers*; Environmental Research Software: Edgewater, MD, 1991.
- (43) Millero, F. J. *Geochim. Cosmochim. Acta* **1985**, *49*, 547–553.
- (44) Fallab, S. Agnew. *Chem. Int. Ed.* **1967**, *6*, 496–507.
- (45) Klausen, J.; Tröber, S. P.; Haderlein, S. B.; Schwarzenbach, R. P. *Environ. Sci. Technol.* **1995**, *29*, 2396–2404.
- (46) Schwarzenbach, R. P.; Stierli, R.; Lanz, K.; Zeyer, J. *Environ. Sci. Technol.* **1990**, *24*, 1566–1574.
- (47) Larson, R. A.; Weber, E. J. *Reaction Mechanisms in Environmental Organic Chemistry*; Lewis Publishers: Boca Raton, FL, 1994; p 199.
- (48) Arakaki, T.; Morse, J. W. *Geochim. Cosmochim. Acta* **1993**, *57*, 9–14.
- (49) Saji, T.; Aoyagui, S. *J. Electroanal. Chem. Interfacial Electrochem.* **1975**, *58*, 401–410.
- (50) Saji, T.; Aoyagui, S. *J. Electroanal. Chem.* **1975**, *63*, 31–37.
- (51) Jolly, W. L. *Modern Inorganic Chemistry*, 2nd ed.; McGraw-Hill: New York, 1991; pp 496–497.
- (52) Morel, F. M. M.; Hering, J. G. *Principles and Applications of Aquatic Chemistry*; Wiley: New York, 1993; pp 332–342.
- (53) Smith, R. M.; Martell, A. E. *Critical Stability Constants*; Plenum Press: New York, 1976.
- (54) Flynn, S. M.; Clydesdale, F. M.; Zajicek, O. T. *J. Food Prot.* **1984**, *47*, 36–40.

Received for review August 5, 1997. Revised manuscript received December 23, 1997. Accepted January 26, 1998.

ES9706864